Supporting Information for

Improved Stability of Polycrystalline Bismuth Vanadate Photoanodes by use of Dual-Layer Thin TiO_2/Ni Coatings

Matthew T. McDowell[1,2], Michael F. Lichterman[1,2], Joshua M. Spurgeon[1,2], Shu Hu[1,2], Ian D. Sharp[3], Bruce S. Brunschwig[4], and Nathan S. Lewis[*1,2,4,5]

[1]Division of Chemistry and Chemical Engineering, 210 Noyes Laboratory, California Institute of Technology, Pasadena, CA, 91125, USA
[2]Joint Center for Artificial Photosynthesis, California Institute of Technology, 1200 E. California Blvd., Pasadena, CA, 91125, USA
[3]Joint Center for Artificial Photosynthesis, Lawrence Berkeley National Laboratory, Berkeley, CA, 94720, USA
[4]Beckman Institute, California Institute of Technology, Pasadena, CA, 91125, USA
[5]Kavli Nanoscience Institute, California Institute of Technology, Pasadena, CA, 91125, USA

A. X-ray diffraction of $BiVO_4$ films.

Figure S1 shows x-ray diffraction patterns of a bare FTO/glass substrate (bottom trace) and of an FTO/glass substrate coated with a spin-cast $BiVO_4$ thin film (top). The $BiVO_4$ film is indexed to the monoclinic phase of the material (space group I2/b, JCPDS no. 01-074-4894).

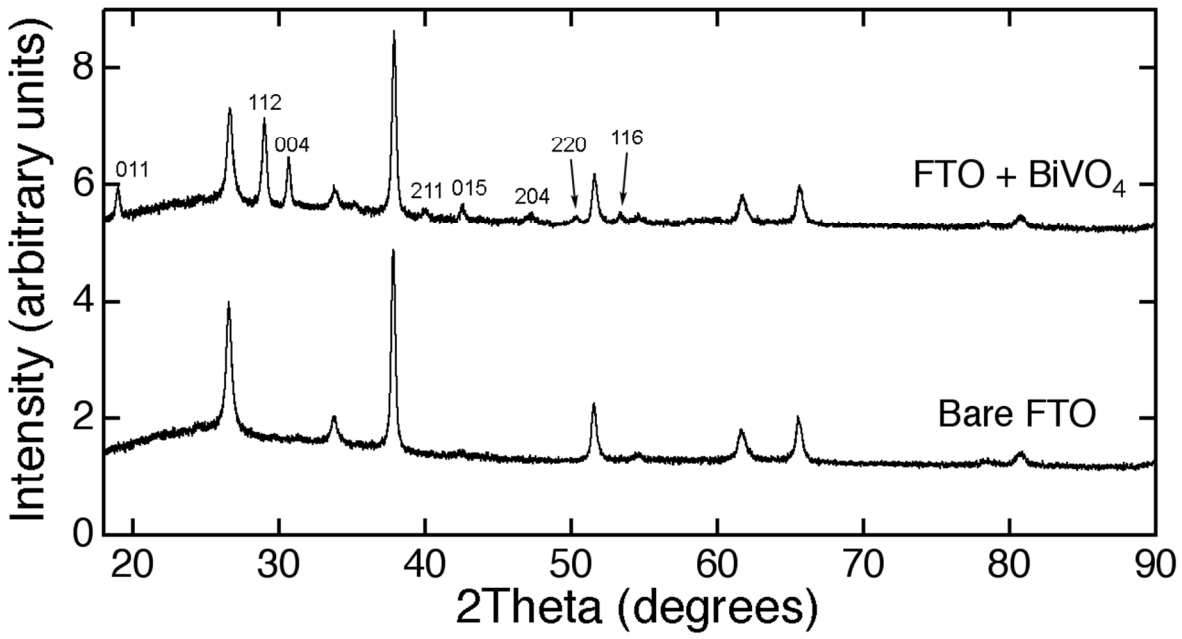

Figure S1. X-ray diffraction scans of bare FTO and FTO with a thin film of $BiVO_4$.

B. Photocorrosion of bare $BiVO_4$ films.

In an experiment to demonstrate the effects of photocorrosion vs. dark dissolution, $BiVO_4$ films on FTO glass were examined before and after either i) soaking in 0.10 M KOH (pH 13), or ii) PEC operation under potentiostatic control at the OER potential under illumination in 0.10 M KOH. Figure S2 shows a photograph of various samples before and after these treatments for different time durations. Samples B and C, which were soaked in pH 13 KOH for 1 h and 15 h, respectively, exhibited a similar dark yellow color to that of the pristine sample (A). In contrast, samples D and E, which were used as electrodes and held at the OER potential in pH 13 KOH, exhibited a paler yellow color. This suggests that photoelectrochemical corrosion processes in pH 13 electrolyte caused a greater change in the thickness or composition than dark dissolution processes.

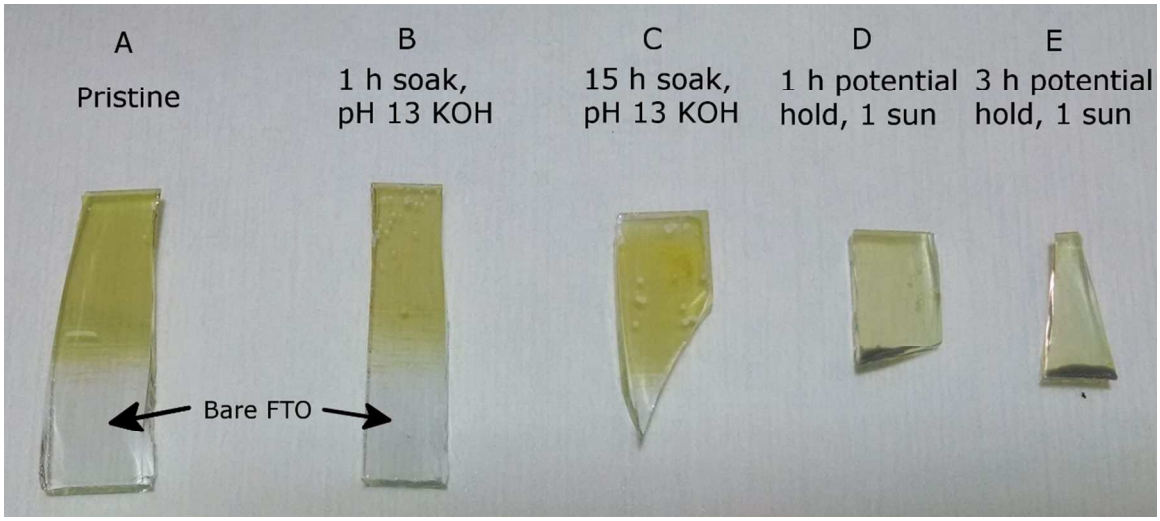

Figure S2. Photograph of various $BiVO_4$ films on FTO glass before (A) and after (B-E) various chemical and photoelectrochemical treatments.

Further qualitative insight into differences between dissolution and photocorrosion was obtained through examination of SEM images of films that were soaked or underwent photoelectrochemical treatment, as shown in Fig. S3 below. The soaked film (B) had a similar continuous morphology to the pristine film (A) albeit with a minor change in roughness, suggesting slight dissolution. The film that had been subjected to photoanodic conditions (C) had a significantly different morphology, with disconnected crystallites as well as the FTO film visible underneath. These images show that corrosion/dissolution processes were much more facile when the films were subject to photooxidation.

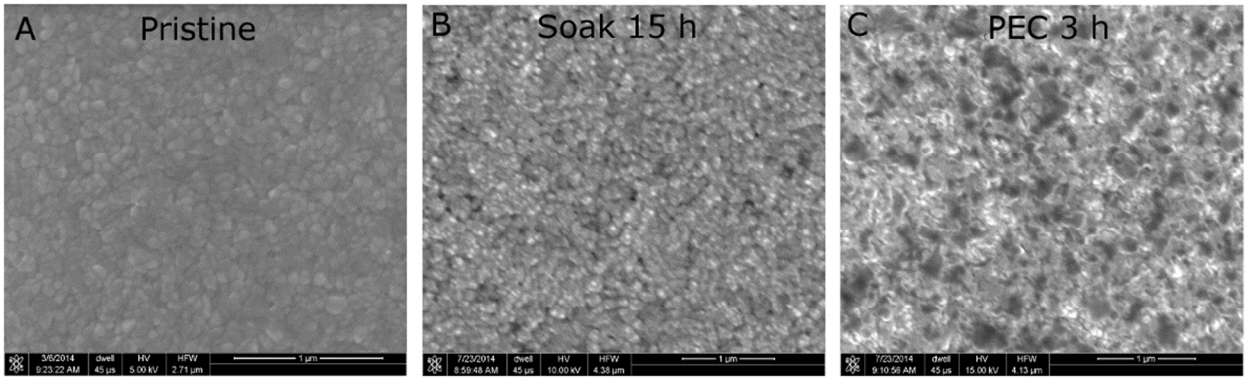

Figure S3. Scanning electron microscopy images of (A) a pristine $BiVO_4$ film, (B) a film that was soaked in 0.10 M KOH for 15 h, and (C) a film that has undergone photoelectrochemical treatment by holding at the OER potential under illumination for 3 h in 0.10 M KOH.

C. Cycling and stability of a $BiVO_4$/Ni sample.

For comparison to the $BiVO_4/TiO_2$/Ni data, samples without the TiO_2 layer were also fabricated and tested. Fig. S4 shows the *J-E* behavior of such a sample at pH = 13, with the Ni sputtered for 30 s directly onto the $BiVO_4$. Fig. S5 shows the photocurrent stability while the anode was under potential control at $E^{o\prime}(O_2/H_2O)$.

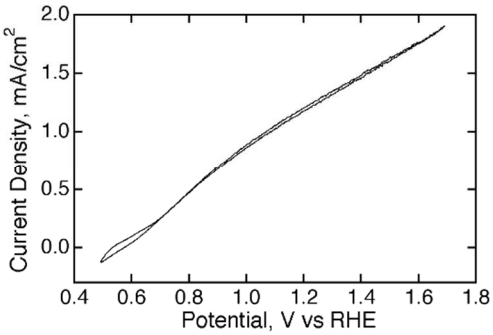

Figure S4. 10th illuminated *J-E* cycle for a sample that consisted of Ni sputtered directly onto $BiVO_4$ (pH 13). The Ni was sputtered for 30 s, which is the same thickness as the Ni in the $BiVO_4/TiO_2$/Ni sample shown in Fig. 2a in the main text.

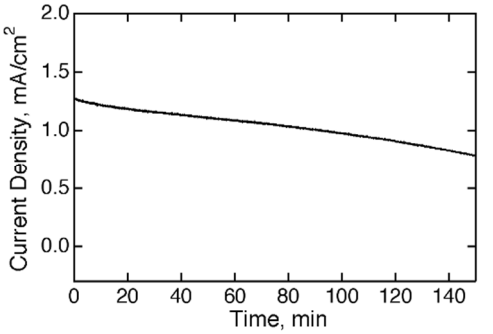

Figure S5. Photocurrent under potentiostatic conditions at the OER potential for the same $BiVO_4$/Ni sample.

In general, such $BiVO_4$/Ni samples showed a decay in photocurrent with time, although their stability was better than that of bare $BiVO_4$ anodes. As discussed in the main text, Ni is converted to catalytically active NiOOH during initial CV cycling. NiOOH is known to be ion-porous,[1] which would allow the underlying $BiVO_4$ to be exposed to electrolyte species, thus facilitating an acceleration of photocorrosion.

D. XPS of bare $BiVO_4$.

Figure S6 shows XPS spectra of a bare $BiVO_4$ electrode before and after 60 illuminated CVs in 0.10 M KOH (pH = 13). The Bi 4f and V 2p peaks are shown. The peaks were similar before and after cycling, although the Bi peak intensity increased slightly and the V peak intensity decreased slightly.

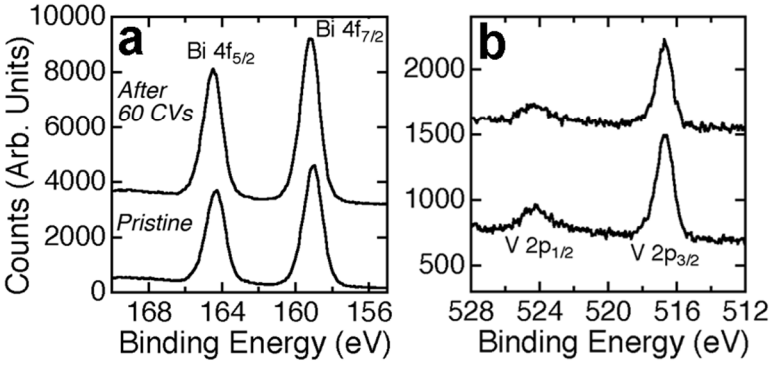

Figure S6. XPS of a bare $BiVO_4$ electrode before and after 60 illuminated *J-E* sweeps in 0.10 M KOH(aq). The 'before' data are the bottom scans, and the 'after' data are the top scans. (a) Bi 4f peaks, (b) V 2p peaks.

E. Photoelectrochemical data from XPS experiments in main text.

Figure S7 shows 60 illuminated *J-E* sweeps in 0.10 M KOH(aq) for the $BiVO_4/TiO_2$ sample whose XPS data are shown in Fig. 4a-c in the main text. 30 ALD cycles were used for this sample.

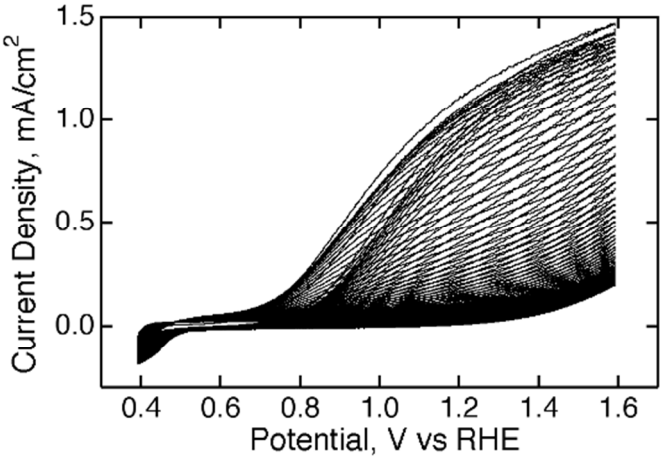

Figure S7. 60 illuminated *J-E* sweeps in 0.10 M KOH(aq) for a $BiVO_4/TiO_2$ sample (the XPS data for this sample are shown in the main text). The photocurrent decreased with cycling.

Figure S8 shows 60 illuminated *J-E* sweeps in 0.10 M KOH(aq) for the $BiVO_4/TiO_2$/Ni sample for which XPS data are shown in Fig. 4d-g in the main text. The TiO_2 layer was deposited with 30 ALD cycles, and the Ni layer was <1 nm thick.

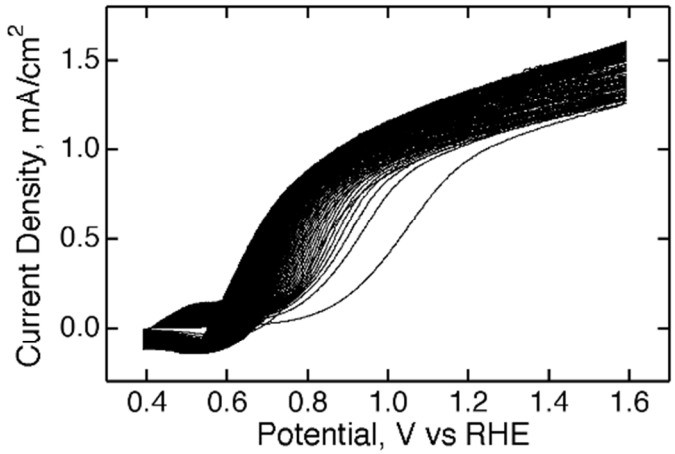

Figure S8. 60 illuminated *J-E* sweeps in 0.10 M KOH(aq) for a $BiVO_4/TiO_2$/Ni sample (the XPS data for this sample are shown in the main text). The photocurrent increased with cycling.

REFERENCES

1. Lin, F.; Boettcher, S. W. *Nature Materials* **2014,** 13, 81-86.